

# Lysozyme Aggregation and Solution Properties Studied Using PGSE NMR Diffusion Measurements

William S. Price,\* Fumihiko Tsuchiya, and Yoji Arata

Contribution from the Water Research Institute, Sengen 2-1-6, Tsukuba, Ibaraki 305-0047, Japan

Received June 30, 1999. Revised Manuscript Received October 19, 1999

**Abstract:** The solution behavior of lysozyme was studied as a function of protein concentration, NaCl concentration, pH, and temperature using pulsed-gradient spin-echo NMR diffusion measurements. The lysozyme solutions clearly exhibited nonideal behavior which was sensitive to both the salt concentration and pH. Lysozyme has an isoelectric point of pH 11, and it is often overlooked that at normal pH it has a net positive charge. Since lysozyme is a charged species, the changes in the diffusion coefficients were interpreted, considering the competing effects of salt-mediated changes in protein interactions (e.g., electrostatic repulsion) and aggregation. The behavior is in agreement with Derjaguin-Landau-Verwey-Overbeek (DLVO)-type modeling, accounting for the attractive and repulsive forces present. The diffusion data was compared with various self-association models, including corrections for the effects of self-obstruction. The diffusion coefficients of the higher oligomers were calculated, assuming that the monomers aggregated as hard spheres. Using an isodesmic association model, the equilibrium constant for the self-association of lysozyme at pH 4.6 and 298 K in the presence of 0.5 M NaCl was estimated to be  $118 \pm 12 \text{ M}^{-1}$ .

## Introduction

The solution behavior of proteins is of fundamental importance to biological systems as well as for understanding the crystallization process.<sup>1</sup> Two important differences between the crystallizing of small molecules and proteins are the phenomenon of protein aggregation and that protein crystallization requires supersaturation ratios higher than those required for crystallizing small molecules.<sup>2</sup> It is generally thought that aggregation is a necessary but poorly understood step in the crystallization process. Except at very low concentrations (and perhaps salt concentrations), many proteins are in some equilibria between different states of aggregation (e.g., monomer  $\leftrightarrow$  dimer  $\leftrightarrow$  higher oligomer). The aggregation process and protein solubility has a complex dependence on pH, temperature, and the protein and salt concentrations. This complex behavior results from intermolecular forces since proteins are both colloids and polymers.<sup>1,3-5</sup>

Lysozyme is one of the most studied of all proteins and its propensity for aggregation, both in unsaturated and supersaturated solutions, has been widely reported. Monomeric lysozyme has a molecular weight of 14 320 dalton and is often taken as being a nearly spherical prolate ellipsoid (i.e.,  $a = 27.5 \text{ \AA}$  and  $b = 16.5 \text{ \AA}$ ).<sup>6</sup> Lysozyme aggregation has been studied with a number of traditional techniques including equilibrium ultracentrifugation,<sup>7,8</sup> dialysis,<sup>9</sup> Gouy interferometry,<sup>10</sup> light and

neutron scattering,<sup>3,11-16</sup> NMR dispersion studies,<sup>17</sup> and, more recently, NMR diffusion measurements.<sup>18</sup> Surprisingly, even after such extensive study, both the equilibria between the different oligomeric states and their aggregation mechanism are far from clarified. We briefly summarize the results of some recent studies reported in the literature. From neutron scattering studies, Boué et al. found that in unsaturated solution the monomer-dimer equilibrium is dominant up to pH 9.<sup>11</sup> They found that the higher order aggregates such as octamers dominate while at high supersaturation. From crystal growth rate data, Li et al.<sup>19</sup> have proposed that the aggregation of lysozyme proceeds by successive addition of monomers to form dimers, the addition of dimers to form tetramers, and so forth. However, studies in supersaturated lysozyme solutions at pH 4 using chemical cross-linking<sup>20</sup> revealed that high ionic strength solutions were highly aggregated and that the aggregates appear

\* Corresponding author: Dr. William S. Price, Water Research Institute, Sengen 2-1-6, Tsukuba, Ibaraki 305-0047, Japan. Telephone: (81-298) 58 6186. FAX: (81-298) 58 6144. E-mail: wprice@wri.co.jp.

(1) De Young, L. R.; Fink, A. L.; Dill, K. A. *Acc. Chem. Res.* **1993**, *26*, 614-620.

(2) Forsythe, E.; Pusey, M. L. *J. Cryst. Growth* **1994**, *139*, 89-94.

(3) Kuehner, D. E.; Heyer, C.; Rämisch, C.; Fornefeld, U. M.; Blanch, H. W.; Prausnitz, J. M. *Biophys. J.* **1997**, *73*, 3211-3224.

(4) Retailleau, P.; Riès-Kautt, M.; Ducruix, A. *Biophys. J.* **1997**, *73*, 2156-2163.

(5) Riès-Kautt, M.; Ducruix, A. *Methods Enzymol.* **1997**, *276*, 23-59.

(6) Dubin, S. B.; Clark, N. A.; Benedek, G. B. *J. Chem. Phys.* **1971**, *54*, 5158-5164.

(7) Kim, H.; Deonier, R. C.; Williams, J. W. *Chem. Rev.* **1977**, *77*, 659-690.

(8) Wills, P. R.; Nichol, L. W.; Siezen, R. J. *Biophys. Chem.* **1980**, *11*, 71-82.

(9) Wilson, L. J.; Adcock-Downey, L.; Pusey, M. L. *Biophys. J.* **1996**, *71*, 2123-2129.

(10) Kim, Y.-C.; Myerson, A. S. *J. Cryst. Growth* **1994**, *143*, 79-85.

(11) Boué, F.; Lefaucheux, F.; Robert, M. C.; Rosenman, I. *J. Cryst. Growth* **1993**, *133*, 246-254.

(12) Giordano, R.; Wanderlingh, F.; Wanderlingh, U.; Teixeira, J. *J. Phys. IV* **1993**, *3*, 237-240.

(13) Eberstein, W.; Georgalis, Y.; Saenger, W. *J. Cryst. Growth* **1994**, *143*, 71-78.

(14) Georgalis, Y.; Schüler, J.; Frank, J.; Soumpasis, M. D.; Saenger, W. *Adv. Colloid Interface Sci.* **1995**, *58*, 57-86.

(15) Muschol, M.; Rosenberger, F. *J. Chem. Phys.* **1995**, *103*, 10424-10432.

(16) Niimura, N.; Minezaki, Y.; Ataka, M.; Katsura, T. *J. Cryst. Growth* **1995**, *154*, 136-144.

(17) Raeymaekers, H. H.; Eisendrath, H.; Verbeke, A.; van Haverbeke, Y.; Muller, R. N. *J. Magn. Reson.* **1989**, *85*, 421-425.

(18) Nesmelova, I. V.; Fedotov, V. D. *Biochim. Biophys. Acta* **1998**, *1383*, 311-316.

(19) Li, M.; Nadarajah, A.; Pusey, M. L. *J. Cryst. Growth* **1995**, *156*, 121-132.

to increase by the addition of monomer units. Hence, as the temperature is decreased and/or the pH and supersaturation increased, the dominant aggregation species shifts from dimer to higher oligomer. The exchange between the different oligomeric states of lysozyme is most likely to be very slow since it has been found<sup>21</sup> that antibody–lysozyme complexes have lifetimes much greater than  $10^3$  s, and it is also well-known that lysozyme solutions can take very long times to reach equilibrium.<sup>4</sup>

Since the aggregation behavior of lysozyme is not well-understood and even its existence disputed, it is less than surprising that the crystallization behavior of lysozyme is also not well clarified.<sup>5,14,22–25</sup> The aggregation and crystallization behaviors of lysozyme are closely linked as it has been reported that the critical nucleus most likely consists of four monomers<sup>25,26</sup> and the growth unit is likely to be the octamer.<sup>11,27,28</sup> This dependence on aggregated states explains not only why high supersaturation ratios are required for lysozyme crystallization but also why the growth rate is a function of the supersaturation, pH, and salt concentration.<sup>2,27</sup>

Electrostatic effects are now realized to be determinants in protein–protein association<sup>29</sup> and in binding interactions between oligonucleotide to single-stranded DNA oligomers.<sup>30</sup> Due to its high isoelectric point (i.e., pH 11), lysozyme has a net positive charge at all of the pHs used in the present study. In low ionic strength solutions, lysozyme interacts mainly through a combination of electrostatic repulsion and attractive dispersion forces.<sup>31</sup> In the process of crystallizing lysozyme, a salt such as NaCl is added, which lowers the electrostatic barriers between protein molecules, thus achieving supersaturation of the protein at lower protein concentrations.<sup>10,13,20</sup> Above 0.5 M NaCl the screening is virtually complete<sup>4,13</sup> and van der Waals interactions prevail. Interestingly, the results of two recent static and dynamic light scattering studies have been interpreted to suggest that no aggregation occurs even at high pH and ionic strength;<sup>3,32</sup> further, it was implied that lysozyme crystallization and precipitation could be explained in terms of a phase transition (which depends on pH, ionic strength, and the type of salt) and not by a gradual change in aggregation state.<sup>3</sup>

The self-diffusion coefficient,  $D$ , has a direct correlation with molecular weight and pulsed-gradient spin–echo (PGSE, also known as pulsed field gradient) NMR<sup>33–35</sup> measures the self-diffusion coefficient, as against dynamic light scattering which

measures the mutual-diffusion coefficient. In the case of a homogeneous species,  $D$  is straightforwardly related to the hydrodynamic properties of the diffusing species. PGSE has found a recent gain in popularity for probing protein and lipid aggregation<sup>36–42</sup> and protein unfolding.<sup>43</sup> NMR  $T_2$  measurements have also been used to study protein aggregation.<sup>44</sup> However, the relationship between the aggregation state and the line width is somewhat ambiguous, and the resonance used for the line width measurements must be carefully chosen.<sup>40</sup>

The aims of the present work were to study the solution and aggregation properties of lysozyme at different pH, temperature, protein and salt (i.e., ionic strength) concentrations using PGSE NMR diffusion measurements. Measurements were performed at lysozyme concentrations of 1.5, 2.8, and 10 mM at various pH values (3, 4.6, 6, and 8), temperatures (283, 288, 293, 298, and 308 K), and NaCl concentrations (0, 0.15, and 0.5 M) to elucidate the effects of these parameters, and the results were compared with some theoretically calculated values for lysozyme diffusion, calculated using the bead model approximation. These three lysozyme concentrations were chosen to display the differences in behavior in undersaturated, saturated, and supersaturated lysozyme solutions. The concentration dependence (up to 5 mM) of the lysozyme diffusion coefficient at pH 4.6 and 298 K in the presence of (1) 0, (2) 0.15, and (3) 0.5 M NaCl was studied in detail and compared with three different association models. The salt concentrations for the lysozyme concentration dependence study were chosen to facilitate comparison with the work of Li et al.<sup>19,28</sup> To the authors' knowledge this is the first detailed study of lysozyme aggregation under various pHs and salt and protein concentrations using PGSE NMR.

### PGSE NMR Measurements of Lysozyme Aggregation

The lysozyme solutions used in the present study are crowded systems in that the average spacing of the lysozyme molecules is much less than the mean-squared displacement of the particles over the time scale of the PGSE diffusion experiment. For example, the average spacing between lysozyme molecules in a 0.5 mM solution (the lowest concentration studied here) is of the order of 9 nm. Yet taking the monomer diffusion coefficient at 298 K to be of the order of  $1 \times 10^{-10}$  m<sup>2</sup> s<sup>-1</sup>, and the time scale of the experiment to be 30 ms, then the mean-squared displacement calculated from the Einstein equation is about 4  $\mu$ m. Thus, during the diffusion measurement there is a high probability for different lysozyme molecules to collide numerous times. This has two consequences; first, even in the absence of aggregation the measured diffusion coefficient of any oligomeric species will decrease due to self-obstruction as the lysozyme concentration increases. Second, there is evidence of an ensemble averaging of the diffusion coefficients of the different

(20) Wang, F.; Hayter, J.; Wilson, L. *J. Acta Crystallogr.* **1996**, D52, 901–908.

(21) Xavier, K. A.; Willson, R. C. *Biophys. J.* **1998**, 74, 2036–2045.

(22) Haas, C.; Drenth, J. *J. Cryst. Growth* **1995**, 154, 126–135.

(23) Noever, D. A. *J. Phys.* **1995**, D28, 1384–1392.

(24) Patro, S. Y.; Przybycien, T. M. *Biophys. J.* **1996**, 70, 2888–2902.

(25) Kierzek, A. M.; Wolf, W. M.; Zielenkiewicz, P. *Biophys. J.* **1997**, 73, 571–580.

(26) Bessho, Y.; Ataka, M.; Asai, M.; Katsura, T. *Biophys. J.* **1994**, 66, 310–313.

(27) Nadarajah, A.; Forsythe, E. L.; Pusey, M. L. *J. Cryst. Growth* **1995**, 151, 163–172.

(28) Nadarajah, A.; Li, M.; Pusey, M. L. *Acta Crystallogr.* **1997**, D53, 524–534.

(29) Camacho, C. J.; Weng, Z.; Vajda, S.; DeLisi, C. *Biophys. J.* **1999**, 76, 1166–1178.

(30) Zhang, W.; Ni, H.; Capp, M. W.; Anderson, C. F.; Lohman, T. M.; Record, M. T., Jr. *Biophys. J.* **1999**, 76, 1008–1017.

(31) Kuehner, D. E.; Blanch, H. W.; Prausnitz, J. M. *Fluid Phase Equilib.* **1996**, 116, 140–147.

(32) Muschol, M.; Rosenberger, F. *J. Cryst. Growth* **1996**, 167, 738–747.

(33) Price, W. S. Gradient NMR. In *Annual Reports on NMR Spectroscopy*; Webb, G. A., Ed.; Academic Press: London, 1996; pp 51–142.

(34) Price, W. S. *Concepts Magn. Reson.* **1997**, 9, 299–336.

(35) Price, W. S. *Concepts Magn. Reson.* **1998**, 10, 197–237.

(36) Lin, M.; Larive, C. K. *Anal. Biochem.* **1995**, 229, 214–220.

(37) Israelachvili, J.; Wennerström, H. *Nature* **1996**, 379, 219–225.

(38) Price, W. S.; Nara, M.; Arata, Y. *Biophys. Chem.* **1997**, 65, 179–187.

(39) Ilyina, E.; Roongta, V.; Pan, H.; Woodward, C.; Mayo, K. H. *Biochemistry* **1997**, 36, 3383–3388.

(40) Mansfield, S. L.; Jayawickrama, D. A.; Timmons, J. S.; Larive, C. K. *Biochim. Biophys. Acta* **1998**, 1382, 257–265.

(41) Price, W. S.; Tsuchiya, F.; Suzuki, C.; Arata, Y. *J. Biomol. NMR* **1999**, 13, 113–117.

(42) Price, W. S.; Tsuchiya, F.; Arata, Y. Protein Aggregation Studies Using PFG NMR Diffusion Measurements. In *Advances in Magnetic Resonance in Food Science*; Belton, P. S., Hills, B. P., Webb, G. A., Eds.; Royal Society of Chemistry: London, 1999; pp 35–42.

(43) Jones, J. A.; Wilkins, D. K.; Smith, L. J.; Dobson, C. M. *J. Biomol. NMR* **1997**, 10, 199–203.

(44) Inoue, T.; Akasaka, K. *J. Biochem.* **1987**, 102, 1371–1378.

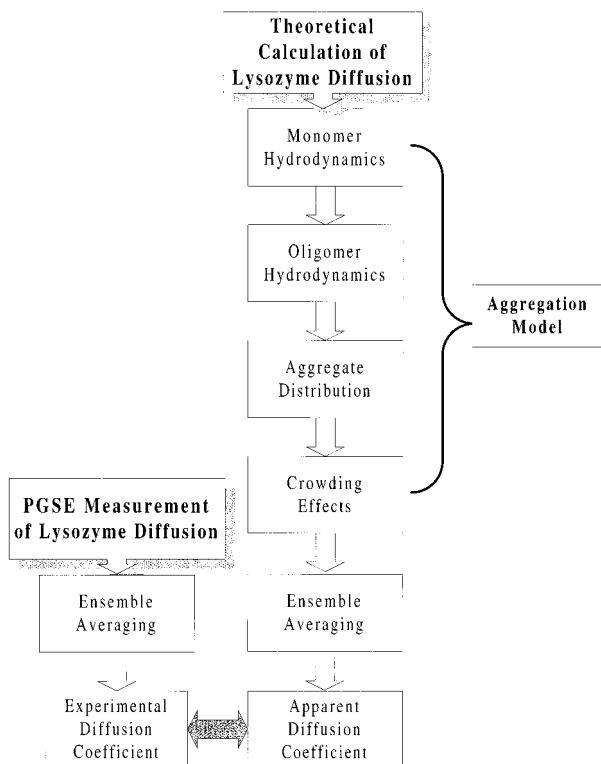


**Figure 1.** Schematic diagram of the procedure for studying lysozyme aggregation using PGSE NMR. The experimentally observed diffusion coefficient,  $\langle D \rangle_w^C$ , is compared to a theoretically calculated value using a model that includes the distribution and shape of the various oligomeric species. The model also includes the effects of ensemble averaging of the oligomeric diffusion coefficients and reduction of the diffusion coefficients due to crowding (i.e., self-obstruction) since both of these effects are inherently included in the diffusion coefficient derived from the PGSE experiment.

oligomers on the microscopic scale that results in a narrower distribution of diffusion coefficients than would be expected for an isolated ensemble of molecules of the same mass distribution. Such an averaging process has been noted in polymer systems.<sup>45</sup> In fact, in all of our measurements only a single “average” diffusion coefficient was observed (N.B. the resonances from the various aggregated states are overlapped in the NMR spectrum).

The measured “apparent” lysozyme diffusion coefficients were analyzed by comparison with theoretically calculated values. The model for calculating the diffusion coefficient starts by considering the distribution and hydrodynamic shape of isolated (i.e., non-interacting in the molecular dynamic sense) aggregating species. The interactions between the species that occur on the time scale of the PGSE experiment (i.e., crowding effects and ensemble averaging) which are inherently included in the observed diffusion coefficient must be explicitly included into the simulated values. The individual steps in calculating the theoretical diffusion coefficient are presented in the following subsections and summarized in Figure 1.

**PGSE NMR Lysozyme Diffusion Measurements. PGSE Measurement.** The salient features of the PGSE NMR diffusion measurement have been presented elsewhere.<sup>34,35</sup> Assuming that relaxation weighting of the intensities of the different oligomeric species can be neglected and that the exchange between these species is slow (i.e., PGSE measurement time scale around tens of milliseconds), then the echo signal amplitude for a species

existing in  $i$  different aggregation states (i.e., monomer, dimer, ...,  $i$ -mer) undergoing isotropic free diffusion is given by

$$S(g) \propto \sum_i M_{0,i} \exp(-\gamma^2 g^2 D_i \delta^2 (\Delta - \delta/3)) \quad (1)$$

where  $M_{0,i}$  denotes the equilibrium magnetization ( $\propto M_{w_i} n_i$ ; where  $M_{w_i}$  is the molar mass of the  $i$ th aggregate species, and  $n_i$  is the number of such molecules present),  $\gamma$  is the gyromagnetic ratio,  $g$  is the magnitude and  $\delta$  is the duration of the magnetic field gradient pulses, and  $\Delta$  is the separation between the leading edges of the gradient pulses. The PGSE NMR data can then be normalized,

$$E = \frac{S(g)}{S(0)} = \frac{\sum_i M_{w_i} n_i \exp(-bD_i)}{\sum_i M_{w_i} n_i} \quad (2)$$

and for brevity we have set  $b = \gamma^2 g^2 \delta^2 (\Delta - \delta/3)$ .

### Ensemble Averaging

For a polydisperse system the signal attenuation as described by eq 2 is multiexponential. However, no deviation from linearity was observed in the current work even for concentrated lysozyme samples, and thus there is some process resulting in ensemble averaging of the diffusion coefficients of the different oligomeric species on the microscopic scale. We approximate the averaging process by taking the cumulant expansion of eq 2 to second order, thereby obtaining

$$\ln(E) = -b\langle D \rangle_w + \frac{b^2}{2} (\langle D^2 \rangle_w - \langle D \rangle_w^2) \quad (3)$$

where  $\langle D \rangle_w$  is the mass-averaged diffusion coefficient defined by

$$\langle D \rangle_w = \frac{\sum_i M_{w_i} n_i D_i}{\sum_i M_{w_i} n_i} \quad (4)$$

The second term in eq 3 (i.e., the “variance”) reflects the degree of polydispersity and may become evident as nonlinearity in the attenuation plot (i.e.,  $\ln(E)$  vs  $b$ ) especially at large values of  $b$ . However, as all the measured attenuation plots were linear, we have analyzed our data by regressing eq 3 (neglecting the quadratic terms) onto the attenuation data. We note that the diffusion coefficients of the lysozyme oligomers (i.e.,  $D_i$ ) inherently contain the effects of crowding (see below). Thus analysis of the PGSE experiment yields the apparent diffusion coefficient,  $\langle D \rangle_w^C$ , where we have introduced the superscript C to denote the inclusion of crowding effects.

Interestingly, although we have justifiably assumed that exchange between the different oligomeric species is slow on the time scale of  $\Delta$ , the final equation for the apparent diffusion coefficient (i.e., eq 3 without the quadratic terms) is, due to the effects of the ensemble averaging, mathematically equivalent to that for the case of fast exchange.

**Theoretical Calculation of the Lysozyme Diffusion Coefficient. Monomer Hydrodynamics.** The Stokes–Einstein relation relates the diffusion coefficient at infinite dilution (N.B. interactions between the diffusing species are ignored),  $D^0$ , of a particle to its molecular shape via a friction coefficient,  $f$ ,

(45) Callaghan, P. T.; Pinder, D. N. *Macromolecules* **1985**, *18*, 373–379.

$$D^0 = \frac{kT}{f} \quad (5)$$

where  $k$  is the Boltzmann constant and  $T$  is temperature. In the simple case of a sphere

$$f = 6\pi R_D \quad (6)$$

where  $R_D$  is the hydrodynamic (or Stokes) radius. However, the lysozyme monomer is not exactly spherical, and in the present work the monomer diffusion coefficient (i.e.,  $D_1^0$ ) was calculated using the three-dimensional structure of lysozyme<sup>46</sup> assuming that the backbone atoms were of equal size ( $\sigma = 5.0$  Å) with the program DIFFC<sup>47</sup> based on the bead model approximation<sup>48</sup> in water (V. V. Krishnan, private communication and Krishnan<sup>49</sup>). These values do not include nonideal effects (e.g., crowding, electrostatic effects, etc.).  $D_1^0$  was also estimated by extrapolation of the experimental diffusion data to infinite dilution (N.B.  $\lim_{c \rightarrow 0} \langle D \rangle_w^c = D_1^0$ ).

**Oligomer Hydrodynamics.** As a first approximation, the monomer–monomer contact in producing oligomers can be regarded as hard-sphere contact,<sup>48,50</sup> and thus the ratio of the diffusion coefficient of an  $i$ -mer,  $D_i^0$ , to that of the monomer can be modeled by

$$\frac{D_i^0}{D_1^0} = \frac{f_1}{f_i} = F_i i^{-1/3} \quad (7)$$

and the values of  $F_i$  for various geometries are given by Teller et al.<sup>50</sup> While there is only one possible geometry for dimer formation, many possibilities exist for higher oligomers. Consequently, we have simplistically taken all oligomers to be hydrodynamically spherical; thus, the friction coefficient increases according to the inverse cube root of the molecular weight. In fact, the friction coefficients calculated from eq 7 for reasonable geometrical possibilities for the oligomeric shapes are all quite close to that obtained for a sphere of equivalent volume.

**Aggregate Distribution.** Two approaches were used for defining the distribution of the different oligomeric sizes present in the lysozyme solutions. The first was to use association constants reported by Li et al.<sup>19,28</sup> for the reaction scheme monomer  $\leftrightarrow$  dimer  $\leftrightarrow$  tetramer  $\leftrightarrow$  ...  $\leftrightarrow$   $i$ -mer. However, their values only apply to the sample conditions used in their experiments (i.e., 2.8 mM lysozyme in 0.5 M NaCl at pH 4.6). The second, more general, approach was to apply two simple models of self-association (for a recent review, see ref 51).

(1) Monomer  $\leftrightarrow$  dimer model.

We have the aggregation scheme



where  $L_1$  and  $L_2$  represent the monomer and dimer, respectively, and  $K_d$  is the equilibrium constant. Let  $C$  be the total lysozyme concentration and  $c_i$  the molar concentration of aggregate  $L_i$ ,

(46) Smith, L. J.; Sutcliffe, M. J.; Redfield, C.; Dobson, C. M. *J. Mol. Biol.* **1993**, 229, 930–944.

(47) Orekhov, V. Yu.; Nolde, D. E.; Golovanov, A. P.; Korzhnev, D. M.; Arseniev, A. S. *Appl. Magn. Reson.* **1995**, 9, 581–588.

(48) García de la Torre, J.; Bloomfield, V. A. *Q. Rev. Biophys.* **1981**, 14, 81–139.

(49) Krishnan, V. V. *J. Magn. Reson.* **1997**, 124, 468–473.

(50) Teller, D. C.; Swanson, E.; De Haën, C. *Methods Enzymol.* **1979**, 61, 103–124.

(51) Martin, R. B. *Chem. Rev.* **1996**, 96, 3043–3064.

and then the conservation of mass equation can be written as

$$C = c_1 + 2c_2 \quad (9)$$

Thus, the mole fraction of the monomer and dimer are given by

$$\alpha_1 = \frac{-1 + \sqrt{1 + 8K_d C}}{4K_d C} \quad (10)$$

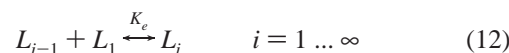
and

$$\alpha_2 = \frac{4K_d C + 1 - \sqrt{1 + 8K_d C}}{4K_d C} \quad (11)$$

respectively.

(2) Isodesmic model.

In this model, aggregates grow by the addition of a monomer,  $L_1$ , unit, thus,



where  $K_e$  ( $= K_2 = K_3 = \dots = K_i$ ) is the equilibrium constant. From the conservation of mass equation we have

$$C = \sum_{i=1}^{\infty} c_i i \quad (13)$$

Thus the mole fraction of the  $i$ -mer is given by

$$\alpha_i = i(K_e C)^{i-1} \left( \frac{2K_e C + 1 - \sqrt{1 + 4K_e C}}{2(K_e C)^2} \right)^i \quad (14)$$

**Crowding Effects.** The effect of crowding (i.e., self-obstruction) on the diffusion process is a complicated many-body problem, and only approximate means of estimating the resulting reduction of the diffusion coefficient,  $f_C$ , exist. We consider two models, the first, a simple model based on scaled particle theory derived by Han and Herzfeld,<sup>52</sup>

$$f_C(v_p) = \frac{D}{D_0} = \exp \left( -\frac{\Delta r}{R} \left( 3 \frac{v_p}{1 - v_p} + \frac{9}{2} \frac{v_p^2}{(1 - v_p)^2} + \frac{9}{4} \frac{v_p^3}{(1 - v_p)^3} \right) \right) \quad (15)$$

In eq 15  $v_p$  is the volume fraction (mL/g) of the protein, and  $\Delta r$  is the step size and  $R$  is the radius of the diffusing particle. From the Smoluchowski equation  $\Delta r/R = 2/3$ .<sup>52</sup> The second model is that of Tokuyama and Oppenheim,<sup>53</sup>

$$f_C(v_p) = \frac{\left( 1 - \frac{9v_p}{32} \right)}{1 + H(v_p) + \frac{(v_p/v_{p0})}{(1 - v_p/v_{p0})^2}} \quad (16)$$

where

(52) Han, J.; Herzfeld, J. *Biophys. J.* **1993**, 65, 1155–1161.

(53) Tokuyama, M.; Oppenheim, I. *Phys. Rev.* **1994**, E 50, R16–R19.

$$H(v_p) = \frac{2b(v_p)^2}{(1-b(v_p))} - \frac{c(v_p)}{(1+2c(v_p))} - \frac{b(v_p)c(v_p)(2+c(v_p))}{(1+c(v_p))(1-b(v_p)+c(v_p))}$$

$$b(v_p) = \sqrt{9v_p/8}$$

$$c(v_p) = 11 v_p/16$$

and

$$v_{p0} = \left(\frac{4}{3}\right)^3 / (7 \ln 3 - 8 \ln 2 + 2)$$

In calculating  $v_p$  we have taken the partial specific volume of lysozyme as 0.75 mL/g. As neither of these models account for the presence of an aggregation process, both models progressively overestimate the reduction in diffusion as the concentration (and degree of aggregation) increases.

**Ensemble Averaging and the Apparent Diffusion Coefficient.** We simulate the ensemble averaging of the diffusion coefficients after calculating the distribution of the oligomeric species and their respective diffusion coefficients using eq 4. Thus, the theoretical apparent diffusion coefficient (see Figure 1) is given by (N.B.  $M_w n_i \propto c_i$ )

$$\langle D \rangle_w^C = \langle D \rangle_w f_C(C) = \frac{\sum_i c_i D_i^0 i^{-1/3}}{C} f_C(C) = \frac{\sum_i \alpha_i D_i^0 i^{-1/3} f_C(C)}{\sum_i \alpha_i D_i^0 i^{-1/3} f_C(C)} \quad (17)$$

## Materials and Methods

**Lysozyme Solution Preparation.** A suitable amount of lysozyme (from chicken egg white, grade 1 L6876; Sigma) was dissolved in aqueous (90%:10%  $^1\text{H}_2\text{O}$ : $^2\text{H}_2\text{O}$ ; pH 4.6) NaCl solution containing 0, 0.15, or 0.5 M NaCl to give a final lysozyme concentration of 0.1 mM and the pH adjusted at room temperature using dilute HCl or NaOH. Each solution was then concentrated  $\sim 10$ -fold using a Centriprep (cutoff MW 3000; Amicon) at room temperature and then redissolved in fresh salt solution of the same salt concentration. This concentrating step was repeated at least three times. Any residual acetate buffer (or other salt) in the lysozyme powder was also removed by this step. The final adjustment of the lysozyme concentration was accomplished by diluting with the appropriate salt solution and by measuring the protein concentration using UV-visible spectroscopy. Two sets of samples were made using this procedure. The first set, for studying the effects of sample conditions (i.e., protein and salt concentrations and pH) on aggregation, were made containing 1.5, 2.8, or 10 mM lysozyme in the presence of 0, 0.15 or 0.5 M salt and at pH values of 3, 4.6, 6, and 8. The second set were made to assess various association models for describing lysozyme aggregation. The second set of samples were in three series at various protein concentrations containing either 0, 0.15, or 0.5 M NaCl at pH 4.6. The sample conditions were chosen to facilitate comparison with previous literature.

Although there is considerable disagreement in the literature regarding the limits of lysozyme solubility,<sup>54,55</sup> the samples containing 1.5 mM lysozyme in 0 and 0.15 M salt should be unsaturated, while those in 0.5 M salt should be saturated only at the highest pH used. The 2.8 mM sample in 0.5 M NaCl will be saturated at pH 4.6 and above, and the samples containing 10 mM lysozyme should be supersaturated in solutions above pH  $\sim 4$  containing 0.15 M salt and above (see Figure 4 in Riès-Kautt and Ducruix<sup>5</sup>). The samples were measured as soon as

(54) Howard, S. B.; Twigg, P. J.; Baird, J. K.; Meehan, E. J. *J. Cryst. Growth* **1988**, *90*, 94.

(55) Cacioppo, E.; Pusey, M. L. *J. Cryst. Growth* **1991**, *114*, 286–292.

possible after preparation to minimize errors associated with precipitation (see below).

**NMR Measurements.**  $^1\text{H}$  NMR experiments were performed at 500 MHz using a Bruker DMX 500 equipped with a 5 mm triple resonance probe with 3-axis shielded magnetic field gradients. In the experiment only the z-gradient was employed, and its strength was first calibrated using the known diffusion coefficient of water.<sup>56</sup> The temperature in the NMR probe was calibrated using methanol or ethylene glycol. Samples ( $\sim 0.2$  mL) for the PGSE experiments were placed into susceptibility-matched microtubes (BMS-005; Shigemi, Tokyo). The stimulated echo pulse sequence with “rectangular” gradient pulses was used to measure the translational diffusion coefficients. Typical acquisition parameters were  $\Delta = 34$  ms and  $\delta = 5$  ms with  $g$  varied up to  $0.64 \text{ T m}^{-1}$ . Low-power presaturation to suppress the water resonance was used during only the last 1.5 s of the recycle delay to minimize any chance of sample heating given some of the samples contained high salt concentrations. In all cases a spectral width of 7.5 kHz was digitized into 32K data points. Each spectrum was the average of 80 transients. A recycle delay of typically 6 s which was sufficient to allow for full relaxation (i.e.,  $> 5 \times T_1$ ) was allowed between each transient. To obtain a sufficient signal-to-noise ratio, the diffusion coefficient of lysozyme was determined using an integral of the aliphatic region (i.e.,  $\sim 0.4$ – $1.7$  ppm). Although this region includes contributions from the (exchangeable) hydroxyl protons of some amino acids (e.g., serine) which have apparent diffusion coefficients greater than that of the protein but less than that of water, their population fraction is too small to have a significant effect on the measured protein diffusion coefficient. Each lysozyme diffusion coefficient is the average of three measurements. In each instance this gave the measured diffusion coefficient with a precision greater than 1% (see the error bars on the relevant figures). However, this should not be viewed as the absolute accuracy of the measurements as it does not include all possible sources of error that may have occurred during sample preparation and so forth. Still the absolute accuracy should be within a few percent. To minimize complications due to NMR relaxation, the delays in the PGSE sequence were kept as short as possible given the magnetic field gradient strengths available.

## Results

**Solvent Diffusion.** Diffusion measurements on the protein-free aqueous solutions showed that the addition of salt at the concentrations used had only a small effect on the water diffusion coefficient and therefore on the solution viscosity. Thus, the changes in the protein diffusion coefficients observed in the presence of different salt concentrations must reflect the changing equilibria of the protein aggregates and protein–protein interactions. The inclusion of 10%  $^2\text{H}_2\text{O}$  reduced the water diffusion coefficient by about 5%.

**The Onset of Aggregation (1.5 mM Lysozyme).** Diffusion measurements were performed at 283, 288, 293, 298, and 308 K on samples containing 1.5 mM lysozyme at pH 3.0, 4.6, 6.0, and 8.0 in the presence of 0, 0.15, and 0.5 M NaCl to investigate the effect of these variables, and the results are summarized together with the monomer diffusion coefficient calculated using the bead model in Figure 2. The diffusion coefficients measured at low pH and in the absence of salt should correspond to that of monomeric lysozyme (i.e., Figure 2A) and consistent with this, the NMR spectra of the lysozyme under these conditions (not shown) had sharp resonances. The theoretical calculations (N.B. infinite dilution) overestimate the experimental monomer diffusion coefficients under these conditions. However, the experimental values inherently contain the effects of crowding, which at this protein concentration, corresponds to reductions of 3.3 or 5.9% from the infinite dilution values, depending on whether the Han and Herzfeld model (eq 15) or Tokuyama and Oppenheim model (eq 16) is used, respectively. At low

(56) Mills, R. J. *Phys. Chem.* **1973**, *77*, 685–688.

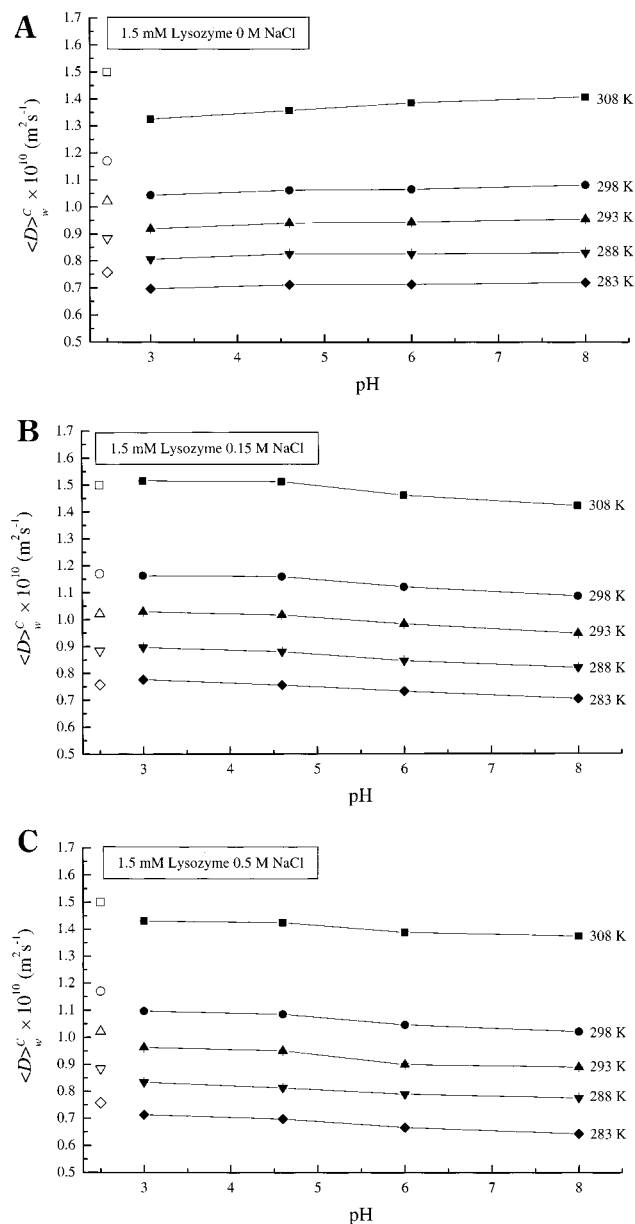


**Figure 2.** Diffusion of 1.5 mM lysozyme versus pH in 90%:10%  $^2\text{H}_2\text{O}$ : $^1\text{H}_2\text{O}$  containing (A) 0, (B) 0.15, and (C) 0.5 M NaCl at 283 K (◆), 288 K (▼), 293 K (▲), 298 K (●) and 308 K (■). The theoretically derived monomer diffusion coefficients calculated by Krishnan and corrected for the increased viscosity due to the  $^2\text{H}_2\text{O}$  content are also shown for comparison (the corresponding open symbols which are arbitrarily positioned at pH 2.5). These theoretical values of the diffusion coefficients do not include corrections for crowding, and correction by the Han and Herzfeld (eq 15) and Tokuyama and Oppenheim models (eq 16) would result in reductions of about 3.3 and 5.9%, respectively, at this protein concentration. The pH 3 data in the absence of salt conform closely to an Arrhenius relation with an activation energy of  $18.6 \text{ kJ mole}^{-1}$ .

temperatures there is only a small increase in the diffusion coefficient with pH. However, at higher temperatures this pH dependence increases. Further, the diffusion coefficients conform to an Arrhenius relationship, as expected for monomeric lysozyme not changing its aggregation state with temperature. The activation energy was determined to be  $18.6 \text{ kJ mole}^{-1}$  which is close to that for the diffusion of pure water over the same temperature range.<sup>57</sup>

Upon addition of 0.15 M NaCl (i.e., Figure 2B) the lysozyme diffusion coefficients increase significantly such that there is now reasonable agreement between the calculated and experimental lysozyme diffusion coefficients at low pH. However, there is now a pronounced negative slope of the diffusion coefficients with increasing pH consistent with the onset of aggregation. In the presence of 0.5 M NaCl (i.e., Figure 2C) the calculated diffusion coefficients again overestimate the experimental lysozyme diffusion coefficients at low pH similar to the case of the salt-free samples, but the diffusion coefficient decreases with pH as in the case of the samples containing 0.15 M NaCl.

**Diffusion of Aggregated Lysozyme (2.8 and 10 mM Lysozyme).** Samples containing 2.8 mM lysozyme in 0, 0.15, and 0.5 M NaCl at pH 3.0, 4.6, 6.0, and 8.0 were measured and the results are shown in Figure 3. At this protein concentration the experimental diffusion coefficient values inherently contain the effects of crowding which should correspond to reductions of 6.3 or 10.9% from the infinite dilution values according to the Han and Herzfeld model (eq 15) or Tokuyama and Oppenheim model (eq 16), respectively. The overall behavior is similar to that observed for the 1.5 mM lysozyme samples except that in the presence of 0.5 M NaCl (Figure 3C) the lysozyme diffusion coefficient appears to increase with pH at the lowest temperatures (i.e., 283 and 288 K). Subsequent observation of the sample revealed that this seemingly incongruous effect results from the aggregation process proceeding to precipitation and crystallization which effectively lowers the “dissolved” lysozyme concentration. The PGSE measurement is insensitive to macroscopic size aggregates by virtue of their extremely short relaxation time, and thus, as the precipitation and crystallization proceeds, the measured diffusion coefficient approaches that expected for a solution with a lower lysozyme concentration.

Supersaturated samples containing 10 mM lysozyme in 0, 0.15, and 0.5 M NaCl at pH 3.0, 4.6, 6.0, and 8.0 were measured, and the results are shown in Figure 4. At this protein concentration the experimental diffusion coefficient values inherently contain the effects of crowding which should correspond to reductions of 24.9 or 36.3% from the infinite dilution values according to the Han and Herzfeld model (eq 15) or Tokuyama and Oppenheim model (eq 16), respectively. At pH 3 all of the measured diffusion coefficients are much lower than the theoretical monomer diffusion coefficients. In the absence of salt (Figure 4A) the measured diffusion coefficients decrease with increasing pH at all of the temperatures measured. However, in the presence of 0.15 M NaCl (Figure 4B), the diffusion coefficients decrease with pH but increase between pH 6 and 8 at all temperatures except for 308 K. In the presence of 0.5 M NaCl (Figure 4C), it was only possible to measure the diffusion coefficients of the samples at 308 K and in some of the low pH samples at the lower temperatures due to the rapid crystallization. In fact even at 308 K, the observed diffusion coefficients increase with pH. The appearance of the spectra (not shown) of the 10 mM lysozyme samples is now extremely pH sensitive with pronounced loss of fine structure with increasing pH. However, the peak positions do not change, which signifies that there are no major structural changes occurring in the lysozyme monomer units. The loss of fine structure is consistent with much longer reorientational correlation times as would be expected for large oligomers.

**Lysozyme Association Models.** Diffusion measurements were performed on lysozyme concentrations up to 5 mM at 298 K and pH 4.6 in the presence of (1) 0, (2) 0.15, and (3) 0.5 M

(57) Price, W. S.; Ide, H.; Arata, Y. *J. Phys. Chem.* **1999**, *103*, 448–450.

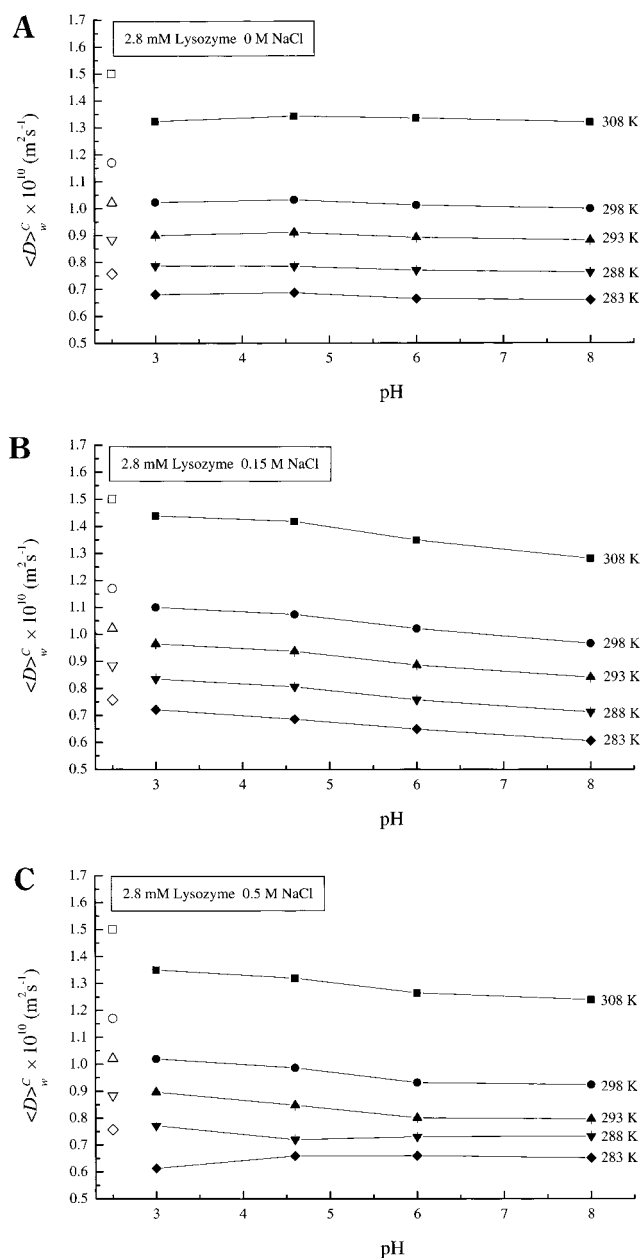


**Figure 3.** Diffusion of 2.8 mM lysozyme versus pH in 90%:10%  $^1\text{H}_2\text{O}$ : $^2\text{H}_2\text{O}$  containing (A) 0, (B) 0.15, and (C) 0.5 M NaCl at 283 K (◆), 288 K (▼), 293 K (▲), 298 K (●) and 308 K (■). The theoretically derived monomer diffusion coefficients calculated by Krishnan and corrected for the increased viscosity due to the  $^2\text{H}_2\text{O}$  content are also shown for comparison (the corresponding open symbols which are arbitrarily positioned at pH 2.5). These theoretical values of the diffusion coefficients do not include corrections for crowding, and correction by the Han and Herzfeld (eq 15) and Tokuyama and Oppenheim models (eq 16) would result in further reductions of about 6.3 and 10.9%, respectively, of the theoretical diffusion coefficients at this protein concentration. At lower temperatures and higher pH the observed diffusion coefficients increase with pH due to lowering of the effective solution lysozyme concentration due to precipitation and crystallization.

NaCl and analyzed by regressing the monomer  $\leftrightarrow$  dimer and isodesmic association models with and without corrections for the effect of crowding (see above and eq 17) onto the data. The regressions also provide estimates of the infinite dilution monomer diffusion coefficient ( $D^0$ ). The results are shown in Figure 5, and the regression results are summarized in Table 1. We purposely only used protein concentrations up to 5 mM to

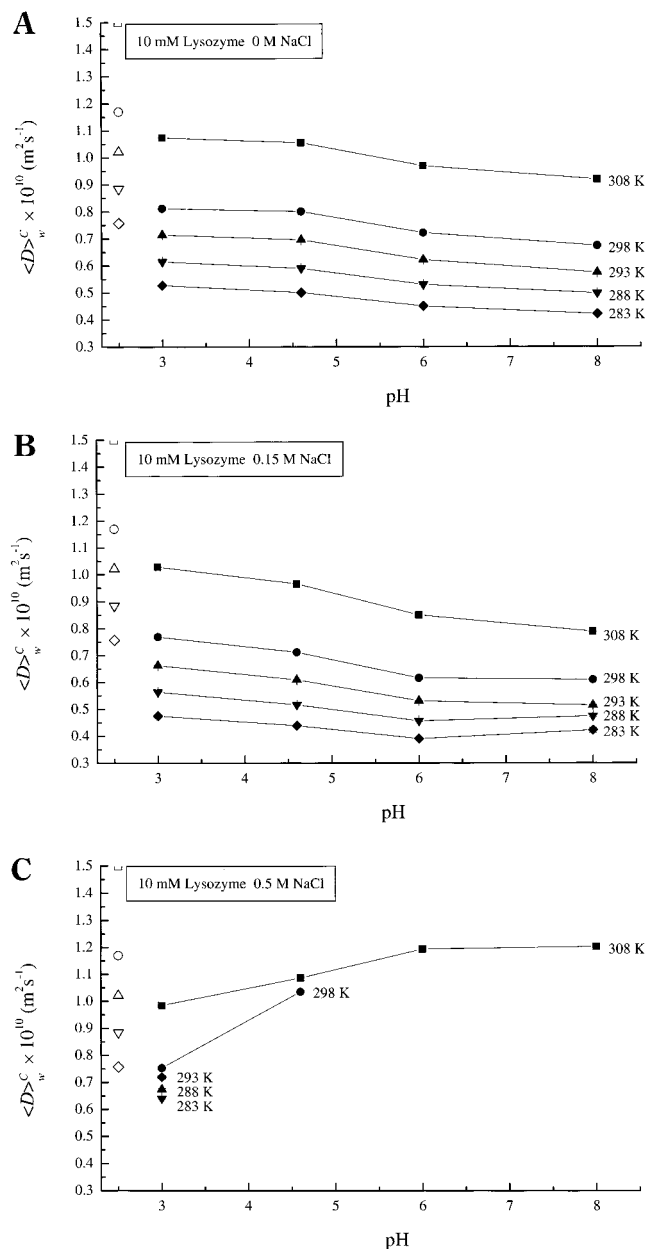


**Figure 4.** Diffusion of 10 mM lysozyme versus pH in 90%:10%  $^1\text{H}_2\text{O}$ : $^2\text{H}_2\text{O}$  containing (A) 0, (B) 0.15, and (C) 0.5 M NaCl at 283 K (◆), 288 K (▼), 293 K (▲), 298 K (●) and 308 K (■). The theoretically derived monomer diffusion coefficients calculated by Krishnan and corrected for the increased viscosity due to the  $^2\text{H}_2\text{O}$  content are also shown for comparison (the corresponding open symbols which are arbitrarily positioned at pH 2.5). These theoretical values of the diffusion coefficients do not include corrections for crowding, and correction by the Han and Herzfeld (eq 15) and Tokuyama and Oppenheim models (eq 16) would result in further reductions of about 24.9 and 36.3%, respectively, of the theoretical diffusion coefficients at this protein concentration. Due to rapid crystallization only measurements at low pH and/or high temperatures were possible. The 308 and 298 K data appears to increase with pH due to the lowering of the effective solution lysozyme concentration due to precipitation and crystallization.

avoid complications due to precipitation (e.g., see above and Figures 3 and 4).

## Discussion

**Lysozyme Aggregation, Diffusion, and Electrostatic Effects.** Some literature values for experimentally determined and theoretically obtained lysozyme diffusion coefficients are sum-

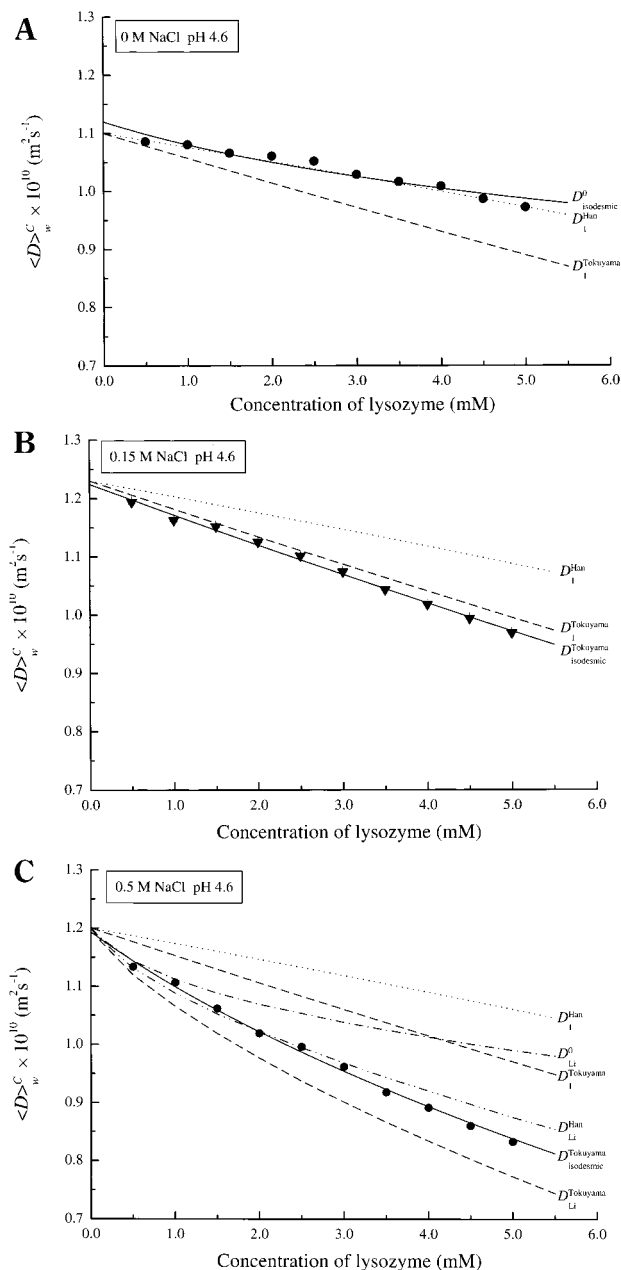


**Figure 5.** Change in lysozyme diffusion coefficients at 298 K and pH 4.6 in the presence of (A) 0 (B) 0.15, and (C) 0.5 M NaCl. The fits of the various aggregation models to the data are summarized in Table 1. In each case the dotted and dashed lines represent the monomer diffusion coefficient at infinite dilution (i.e.,  $D_1^0$  determined from the respective best fitting association model; see Table 1) corrected using the Han and Herzfeld (eq 15) and Tokuyama and Oppenheim (eq 16) corrections, respectively. Clearly in the presence of 0.5 M NaCl the lysozyme must undergo a self-association process as the experimental diffusion coefficient is considerably smaller than the crowding effect corrected (with either model) monomer diffusion coefficient. In the absence of salt (i.e., graph A) the monomer diffusion coefficient corrected with the Han and Herzfeld model gave a good fit to the data. Also shown in this graph is the fit of the isodesmic model without crowding correction (solid line). In the presence of 0.15 M NaCl (i.e., graph B) the best fit to the data was obtained using the isodesmic model in conjunction with the Tokuyama and Oppenheim correction (solid line). In the presence of 0.5 M salt (i.e., graph C) the best fit to the data was obtained using the isodesmic model in conjunction with the Tokuyama and Oppenheim correction (solid line). Also shown in graph (C) are simulations based on the association constants reported by Li et al.<sup>19,28</sup> (---) with Han and Herzfeld correction (---) and Tokuyama and Oppenheim correction (---)

marized in Table 2. Some of the theoretical calculations include a hydration layer since representing the protein by surface coordinates alone often results in the calculated frictional coefficient being too small (e.g., see the review by Byron<sup>58</sup>), however, NMR dispersion and NOE measurements strongly mediate against the existence of a hydration shell.<sup>59</sup> Thus, alternate explanations for the discrepancy between protein structure and hydrodynamic properties are insufficient consideration of (1) the rugosity of the protein surface, (2) crowding effects, and (3) electrostatic interactions (see below). From the data in Table 2 it can be seen that there is some discrepancy between the diffusion coefficients and this probably originates from the different theoretical or experimental conditions employed (i.e., pH, salt and protein concentrations) and inaccurate temperature calibration, especially in the NMR derived values.<sup>35</sup> Nevertheless, the diffusion coefficients obtained for lysozyme in the present work under experimental conditions where it is likely to be monomeric (i.e., the 1.5 mM lysozyme samples at low pH values in Figure 2) are quite comparable to the literature values. The coefficients in Table 2 should also be compared with the estimates of  $D_1^0$  obtained in Table 1. Since the  $D_1^0$  values correspond to infinite dilution conditions, their values are higher than most of the literature estimates of lysozyme diffusion.

Of particular interest is the significant increase and then decrease in the diffusion coefficient of monomeric lysozyme with salt concentration (i.e., compare the pH 3 samples in the presence of 0, 0.15, and 0.5 M NaCl; Figure 2A–C) and the pH-dependent increase at low salt concentrations and decrease at higher salt concentrations (Figure 2A–C). From the very slight change in water diffusion coefficients over this range of salt concentration, it can be realized that the change in the lysozyme diffusion coefficient is not a result of changing solvent viscosity, nor is it a consequence of a large conformational change as is evident from the invariance of the chemical shifts of most of the resonances (e.g., see ref 60) since a large conformational change would significantly change the electronic shielding of the atoms in the lysozyme and bring about significant chemical shift changes. In fact, the invariance of the lysozyme chemical shifts over all of the sample conditions provides justification for the simplistic approach used in modeling the hydrodynamics of the different oligomers in terms of the monomeric shape. If, however, the lysozyme molecules became less folded, this would appear as a hydrodynamically larger volume with a correspondingly smaller diffusion coefficient (see eq 5, in which case our modeling of the data would overestimate the degree of aggregation present).

The increase and decrease in the diffusion coefficient with salt concentration is explained by considering electrostatic interactions between lysozyme molecules and the (polar) solvent (= water + salt) and between themselves. First, we note that a moving charged body tends to orient solvent molecules in its vicinity. This results in a relaxation force on the ion which is equivalent to an additional frictional force.<sup>61</sup> As noted by Bockris and Reddy<sup>61</sup> this effect can be quite significant, and such effects have certainly been noted in electrophoretic experiments of DNA fragments<sup>62</sup> and lysozyme.<sup>63</sup> Second, at

(58) Byron, O. *Biophys. J.* **1997**, *72*, 408–415.

(59) Denisov, V. P.; Halle, B. *J. Mol. Biol.* **1995**, *245*, 682–697.

(60) Bhattacharjya, S.; Balaram, P. *Proteins* **1997**, *29*, 492–507.

(61) Bockris, J. O.; Reddy, A. K. N. *Modern Electrochemistry*; Plenum Press: New York, 1998.

(62) Allison, S. A.; Potter, M.; McCammon, J. A. *Biophys. J.* **1997**, *73*, 133–140.

(63) Allison, S. A.; Wang, H.; Laue, T. M.; Wilson, T. J.; Wooll, J. O. *Biophys. J.* **1999**, *76*, 2488–2501.



**Table 1.** Summary of the Regression of the Monomer–Dimer and Isodesmic Association Models (with and without Crowding Correction) onto the 298 K pH 4.6 Lysozyme Diffusion Data<sup>a</sup>

| NaCl (M) | model                           | crowding correction <sup>b</sup> | $D_1^0$ ( $\text{m}^2 \text{s}^{-1} \times 10^{-10}$ ) | $K_d$ or $K_e$ ( $\text{M}^{-1}$ ) | remarks/fit |
|----------|---------------------------------|----------------------------------|--|------------------------------------|-------------|
| 0        | monomer $\leftrightarrow$ dimer | none                             | 1.13 $\pm$ 0.06  | 241 $\pm$ 338                      | poor        |
|          | monomer $\leftrightarrow$ dimer | Han                              | 1.10 $\pm$ 0.00  | -0.2 $\pm$ 3                       | unphysical  |
|          | monomer $\leftrightarrow$ dimer | Tokuyama                         | 1.12 $\pm$ 0.01  | -20 $\pm$ 1                        | unphysical  |
|          | isodesmic                       | none                             | 1.12 $\pm$ 0.01  | 101 $\pm$ 15                       | poor        |
|          | isodesmic                       | Han                              | 1.10 $\pm$ 0.00  | -0.2 $\pm$ 3                       | unphysical  |
|          | isodesmic                       | Tokuyama                         | 1.11 $\pm$ 0.00  | -30 $\pm$ 2                        | unphysical  |
| 0.15     | monomer $\leftrightarrow$ dimer | none                             | 1.20 $\pm$ 0.28  | 364 $\pm$ 2311                     | poor        |
|          | monomer $\leftrightarrow$ dimer | Han                              | 1.25 $\pm$ 0.04  | 193 $\pm$ 155                      | reasonable  |
|          | monomer $\leftrightarrow$ dimer | Tokuyama                         | 1.22 $\pm$ 0.00  | 10 $\pm$ 4                         | v. good     |
|          | isodesmic                       | none                             | 1.29 $\pm$ 0.03  | 335 $\pm$ 75                       | poor        |
|          | isodesmic                       | Han                              | 1.23 $\pm$ 0.01  | 81 $\pm$ 10                        | reasonable  |
|          | isodesmic                       | Tokuyama                         | 1.22 $\pm$ 0.00  | 10 $\pm$ 3                         | v. good     |
| 0.5      | monomer $\leftrightarrow$ dimer | none                             | 1.09 $\pm$ 0.48  | 391 $\pm$ 4736                     | poor        |
|          | monomer $\leftrightarrow$ dimer | Han                              | 1.16 $\pm$ 0.25  | 382 $\pm$ 2273                     | poor        |
|          | monomer $\leftrightarrow$ dimer | Tokuyama                         | 1.20 $\pm$ 0.08  | 313 $\pm$ 555                      | v. good     |
|          | isodesmic                       | none                             | 1.34 $\pm$ 0.03  | 1056 $\pm$ 173                     | poor        |
|          | isodesmic                       | Han                              | 1.23 $\pm$ 0.02  | 315 $\pm$ 51                       | reasonable  |
|          | isodesmic                       | Tokuyama                         | 1.19 $\pm$ 0.01  | 118 $\pm$ 12                       | v. good     |

<sup>a</sup> To enable comparison of the infinite dilution lysozyme monomer diffusion coefficients ( $D_1^0$ ) with the literature values for lysozyme diffusion given in Table 2, the  $D_1^0$  values in this table should be multiplied by 1.05 to convert them to the values that would be observed in pure  $^1\text{H}_2\text{O}$  water ( $D_{\text{H}_2\text{O}}^0$ ). <sup>b</sup> Han = Han and Herzfeld correction, Tokuyama = Tokuyama and Oppenheim correction.

**Table 2.** Selected Literature Values of Lysozyme Diffusion ( $D_{\text{Lit}}$ ) and Their Respective Experimental/Calculation Conditions<sup>a,b</sup>

| Lys (mM) | temp (K) | salt (M) | solvent                       | pH  | $D_{\text{Lit}}$ ( $\text{m}^2 \text{s}^{-1} \times 10^{-10}$ ) | $D_{\text{H}_2\text{O}}^1$ ( $\text{m}^2 \text{s}^{-1} \times 10^{-10}$ ) | hydration    | method <sup>b</sup> | reference   |
|----------|----------|----------|-------------------------------|-----|---|---|--------------|---------------------|---|
| ID       | 293      |          | H <sub>2</sub> O              | 4.2 | 1.02  | 1.02  |              | LS                  | Eberstein et al. <sup>13</sup>                    |
| ID       | 293      |          | H <sub>2</sub> O              |     | 1.33  | 1.33  | no hydration | C                   | Venable and Pastor <sup>69</sup>                  |
| ID       | 293      |          | H <sub>2</sub> O              |     | 1.08  | 1.08  | hydrated     | C                   | Venable and Pastor <sup>69</sup>                  |
| 0.7      | 293      | 0.1      | H <sub>2</sub> O              | 4.2 | 1.06  | 1.06  |              | LS                  | Dubin et al. <sup>6</sup>                         |
| 0.7      | 293      | 0        | <sup>2</sup> H <sub>2</sub> O | 5.5 | 1.01  | 1.24  |              | PGSE                | Ilyina et al. <sup>39</sup>                       |
| ID       | 298      |          | H <sub>2</sub> O              |     | 1.23  | 1.23  | no hydration | C                   | Krishnan <sup>49</sup> and personal communication |
| 1.4      | 298      | 0.34     | H <sub>2</sub> O              | 4.6 | 1.03  | 1.03  |              | LS                  | Mikol et al. <sup>70</sup>                        |
| 2.0      | 298      | 0.03     | <sup>2</sup> H <sub>2</sub> O | 2.3 | 1.09  | 1.32  |              | PGSE                | Altieri et al. <sup>71</sup>                      |
| 4.2      | 298      | 0        | H <sub>2</sub> O              | 5.6 | 1.15  | 1.15  |              | LS                  | Dubin et al. <sup>72</sup>                        |

<sup>a</sup> To allow easier comparison, the experimental lysozyme diffusion coefficients corrected to reflect diffusion in pure  $^1\text{H}_2\text{O}$  water ( $D_{\text{H}_2\text{O}}^1$ ) are also given. <sup>b</sup> C = calculated; ID = infinite dilution; LS = light scattering.

low pH in the absence of salt, the lysozyme molecules are highly charged and therefore repulsive toward one another, and thus they effectively exclude other molecules from diffusing in their neighborhood (i.e., the self-obstruction effect is increased due to electrostatic interactions); as the ionic strength increases, this effect is decreased, and thus the diffusion coefficient increases (i.e., compare the results for the 0 and 0.15 M NaCl samples). This repulsion has also been suggested from light scattering measurements of lysozyme solutions.<sup>12</sup> This also explains why, in the absence of salt, the diffusion coefficient increases with pH since the charge on lysozyme molecules is reduced. Thus, these colloidal properties help to explain the lysozyme aggregation process. As noted by De Young et al.<sup>1</sup> the aggregation of colloidal particles can be described in the framework of DLVO theory.<sup>3,5,64–66</sup> In particular, there is a shift from net repulsion between monomers at low pH and ionic strength to attraction as the pH and/or ionic strength is increased (N.B. the diffusion coefficient increases with pH at low ionic strength see Figure 2A). At low ionic strength the protein molecules interact through a balance of electrostatic repulsion and attractive dispersion forces. As the ionic strength increases, the macromolecular

Coulombic interactions are essentially screened, and there is overall attraction between species.<sup>3</sup> Thus, at high salt concentrations the energy barriers between the lysozyme molecules are sufficiently reduced so that aggregation can occur. In fact, Ducruix et al.<sup>67</sup> have reported that the net interaction between lysozyme molecules (7 mM, pH 4.5) becomes attractive above 0.25 M NaCl, and Giordano et al.<sup>12</sup> have found from light scattering measurements that attraction dominates close to the isoelectric point. Thus, while the increased charge shielding allows for faster diffusion at intermediate ionic strengths, at even higher ionic strengths (i.e., the 0.5 M sample) the increase in diffusion coefficient is offset by the increasing propensity for aggregation (and therefore slower diffusion) as the molecules are able to more closely approach one another.<sup>1,4,5,13</sup> Using these concepts the data in Figure 2 can now be understood. Our findings are also consistent with the report that the rate at which lysozyme monomers cross a dialysis membrane increases with salt concentration.<sup>68</sup>

(67) Ducruix, A.; Guilleateau, J. P.; Riès-Kautt, M.; Tardieu, A. *J. Cryst. Growth* **1996**, *168*, 28–39.

(68) Wilson, L. J.; Pusey, M. L. *J. Cryst. Growth* **1992**, *122*, 8–13.

(69) Venable, R. M.; Pastor, R. W. *Biopolymers* **1988**, *27*, 1001–1014.

(70) Mikol, V.; Hirsch, E.; Giegé, R. *J. Mol. Biol.* **1990**, *213*, 187–195.

(71) Altieri, A. S.; Hinton, D. P.; Byrd, R. A. *J. Am. Chem. Soc.* **1995**, *117*, 7566–7567.

(72) Dubin, S. B.; Lunacek, J. H.; Benedek, G. B. *Proc. Natl. Acad. Sci. U.S.A.* **1967**, *57*, 1164–1171.

(64) Hunter, R. J. *Foundations of Colloid Science*; Oxford University Press: Oxford, 1986.

(65) Imhof, A.; van Blaaderen, A.; Maret, G.; Mellema, J.; Dhont, J. K. *J. Chem. Phys.* **1994**, *100*, 2170–2181.

(66) Velev, O. D.; Kaler, E. W.; Lenhoff, A. M. *Biophys. J.* **1998**, *75*, 2682–2697.

We note that the  $D_1^0$  values given in Table 1, although free from crowding effects, are affected by electrostatic interactions between the protein and the solvent and this is reflected in the estimates of  $D_1^0$  with the different salt concentrations in Table 1 and also from the data in Figure 2 – Figure 4.

**Lysozyme Aggregation.** Since electrostatic effects (and consequently pH and salt concentration) in part determine the monomer diffusion coefficient, we chose to float  $D_1^0$  when regressing the association models onto the lysozyme diffusion data. The results of the concentration dependence of the lysozyme diffusion experiments show that in the absence of salt, there is apparently little, if any, aggregation as is evident from Figure 5A where the monomer diffusion coefficient corrected for crowding (i.e.,  $D_1^C$ ) using the Han and Herzfeld model agrees very well with the measured diffusion coefficients. In fact neither of the aggregation models either with or without crowding correction was able to satisfactorily fit the data. We note that there is significant disagreement between the two crowding correction models with Tokuyama and Oppenheim's model underestimating the observed diffusion. It should also be stressed that neither model accounts for the effects of aggregation, and thus both corrections progressively overestimate the correction required as the association equilibrium shifts from the monomer to higher oligomers.

In the presence of 0.15 M NaCl the diffusion coefficients decreased more quickly with increasing lysozyme concentration than in the salt-free case. While the monomer diffusion corrected with the Tokuyama and Oppenheim model slightly overestimates the measured diffusion coefficients, the Han and Herzfeld correction now significantly overestimates the diffusion. Thus, it is reasonable to assume that there is some degree of self-association present at the higher protein concentrations. In particular, it was found that both the monomer  $\leftrightarrow$  dimer and isodesmic models coupled with the Tokuyama and Oppenheim correction well-described the experimental data giving  $K_d = 10 \pm 4 \text{ M}^{-1}$  and  $K_e = 10 \pm 3 \text{ M}^{-1}$ , respectively. Our values are considerably smaller than the value ( $208 \text{ M}^{-1}$ ) determined by Raeymaekers et al.<sup>17</sup> using dispersion measurements although we note that their experimental conditions were quite different (0.15 M KCl, 277 K).

In the presence of 0.5 M NaCl, the lysozyme diffusion coefficient decreases much more quickly, and the monomer diffusion corrected with either the Tokuyama and Oppenheim or Han and Herzfeld corrections seriously overestimates the diffusion. Thus, the presence of an aggregation process and higher oligomeric states is certain. The best fit to the data being provided by the isodesmic model in combination with the Tokuyama and Oppenheim correction giving  $K_e = 118 \pm 12 \text{ M}^{-1}$ . This value is considerably smaller than that obtained by Nesmelova and Fedotov ( $K_e = 264.5 \pm 0.5 \text{ M}^{-1}$ );<sup>18</sup> however, their experimental conditions were somewhat different (i.e., no salt and 303 K). Our results agree reasonably well with the equilibria proposed by Li et al.,<sup>19,28</sup> provided that some allowance is given for crowding correction. In particular correction with the Han and Herzfeld model results in an overestimate of the observed diffusion coefficients, whereas correction with Tokuyama and Oppenheim's model underestimates the diffusion coefficient. Further, the equilibria reported

by Li et al. predict a decrease in the gradient of the diffusion coefficient with concentration, whereas our data has a more linear dependence on concentration.

Muschol and Rosenberger have stated that all of the observed changes in protein diffusivity and the results of light scattering studies in both under- and supersaturated lysozyme solutions can be explained in terms of salt-mediated changes in monomeric protein interactions.<sup>32</sup> While our results show that the salt-mediation of protein interactions is a very potent force in determining the lysozyme diffusivity, our results also show that aggregation does occur at sufficiently high salt and protein concentrations. Further, only aggregation could explain the large changes of line width with pH in concentrated lysozyme solution. It would be of interest to conduct diffusion measurements on mutant lysozyme systems with different isoelectric points. Since in the presence of low salt concentrations the decrease in diffusion coefficient can be explained in terms of crowding effects only (i.e., without aggregation), it is reasonable to presume that under these solution conditions that a phase change is involved in the production of macroscopic aggregates (i.e., precipitation) as reported by Kuehner et al.<sup>3</sup> However, at higher salt concentrations our results show that there is certainly some progression through higher oligomeric states prior to precipitation.

## Concluding Remarks

The results of the present diffusion measurements show that the aggregation state and protein interactions are very sensitive to the experimental conditions (i.e., protein and salt concentrations, pH, and temperature) due to both the colloidal and polymeric properties of lysozyme. The Stokes–Einstein equation (i.e., eq 5), which neglects nonideal effects, must be used cautiously in trying to understand the diffusion behavior of aggregating lysozyme solutions due to the presence of nonideal effects such as crowding and electrostatic interactions. The interpretation of PGSE data for studying protein aggregation is strongly dependent on the model used for crowding correction. The analysis would greatly benefit from better models to account for crowding in aggregated systems and of more sophisticated approaches for calculating friction coefficients that include electrostatic contributions.

Even though the resonances of all of the different oligomeric species of lysozyme overlap and consequently, only information on the average molecular weight can be obtained from the diffusion coefficient, the measurements provide a great deal of information on the protein interactions and aggregation which is invaluable for discriminating between aggregation models. The results provide clear evidence for lysozyme aggregation at high salt concentrations and that the association process changes depending on the solution conditions (i.e., salt concentration).

**Acknowledgment.** Professor Bertil Halle (University of Lund) and Dr. Peter Schuck (NIH) are thanked for useful discussions. Dr. V. V. Krishnan (Lawrence Livermore National Laboratory) is thanked for performing the theoretical calculations of lysozyme diffusion.